ADVANCED FUNCTIONAL MATERIALS
www.afm-journal.de

Materials Views
www.MaterialsViews.com

Giant Flexoelectric Polarization in a Micromachined Ferroelectric Diaphragm

Zhihong Wang, Xi Xiang Zhang, Xianbin Wang, Weisheng Yue, Jingqi Li, Jianmin Miao, and Weiguang Zhu**

The coupling between dielectric polarization and strain gradient, known as flexoelectricity, becomes significantly large on the micro- and nanoscale. Here, it is shown that giant flexoelectric polarization can reverse remnant ferroelectric polarization in a bent $Pb(Zr_{0.52}Ti_{0.48})O_3$ (PZT) diaphragm fabricated by micromachining. The polarization induced by the strain gradient and the switching behaviors of the polarization in response to an external electric field are investigated by observing the electromechanical coupling of the diaphragm. The method allows determination of the absolute zero polarization state in a PZT film, which is impossible using other existing methods. Based on the observation of the absolute zero polarization state and the assumption that bending of the diaphragm is the only source of the self-polarization, the upper bound of flexoelectric coefficient of PZT film is calculated to be as large as 2.0×10^{-4} C m^{-1}. The strain gradient induced by bending the diaphragm is measured to be on the order of 10^2 m^{-1}, three orders of magnitude larger than that obtained in the bulk material. Because of this large strain gradient, the estimated giant flexoelectric polarization in the bent diaphragm is on the same order of magnitude as the normal remnant ferroelectric polarization of PZT film.

1. Introduction

Recent studies have demonstrated that epitaxial strain can induce or enhance dielectric polarization (ferroelectricity) in thin films.[1–3] On the contrary, the contribution of the strain gradient to polarization (flexoelectricity) has not been well understood in thin film systems.[4]

Dr. Z. Wang, Dr. X. X. Zhang, Dr. X. Wang, Dr. W. Yue, Dr. J. Li
Advanced Nanofabrication Core Lab
King Abdullah University of Science and Technology
Thuwal 23955-6900, Kingdom of Saudi Arabia
E-mail: zhihong.wang@kaust.edu.sa
Prof. J. Miao
School of Mechanical and Aerospace Engineering
Nanyang Technological University
Singapore 639798
Prof. W. Zhu
School of Electrical and Electronic Engineering
Nanyang Technological University
Singapore 639798
E-mail: ewzhu@ntu.edu.sg

DOI: 10.1002/adfm.201200839

Flexoelectricity is a fundamental physical phenomenon in the dielectrics of any crystal structure, even those with centrosymmetric lattices.[5] The direct flexoelectric effect describes the electric polarization induced by an applied strain gradient. The linear coupling relationships can be written as[6]

$$P_l = \mu_{ijkl} \frac{\partial S_{ij}}{\partial x_k} \quad (1)$$

where P_l is the flexoelectric polarization, μ_{ijkl} the flexoelectric coefficient, x_k the position coordinate, and S_{ij} the elastic strain. Tagantsev's theoretical model indicates that the flexoelectric coefficient is linearly proportional to the dielectric susceptibility, χ_{ij}.[5,6] It takes the form

$$\mu_{ijkl} = \gamma_{kl} \chi_{ij} \frac{e}{a} \quad (2)$$

where γ_{kl} is a constant related to the composition of the material, e is the electron charge, and a is the lattice parameter.

The early literature did not inspire confidence in the application of flexoelectricity because the flexoelectric coefficients, μ_{ijkl}, were trivially small ($\mu_{ijkl} \approx 10^{-10}$ C m^{-1}) and the strain gradient that could be obtained in bulk materials was also limited. However, Tagantsev's prediction that flexoelectric coefficients scale with the dielectric susceptibility motivated Cross and co-workers to investigate the flexoelectric coefficient of high permittivity bulk perovskites, such as $Ba_{0.67}Sr_{0.33}TiO_3$,[7,8] $Pb(Zr,Ti)O_3$,[9,10] and $Pb(Mg_{1/3}Nb_{2/3})O_3$.[11,12] Surprisingly, they found that the coefficient is actually very large ($\mu_{ijkl} \approx 10^{-4}$ C m^{-1}).[7] Their work suggested that the flexoelectric effect could be exploited in real devices, stimulating successive experimental and theoretical work.[13–17]

Published data now suggest that the direct flexoelectric effect may affect the properties of epitaxial thin films in which the lattice mismatch can give rise to very steep elastic strain gradients.[18,19] Catalan and co-workers[18] reported that, in a lattice-mismatched epitaxial ferroelectric thin film made of $Ba_{0.5}Sr_{0.5}TiO_3$, strain relaxation can lead to a smooth, continuous gradient across the film thickness. The out-of-plane strain on the order of 1% at the film/substrate interface may vanish across a thickness of hundreds of nanometers. Obviously, this inhomogeneous strain can generate a tremendous strain gradient on the order of 10^4 m^{-1}, which is 4 to 5 orders

of magnitude higher than the strain gradient that can be obtained from a bulk structure. Recently, Lee and co-workers[19] also reported that the measured strain gradient can be as large as 10^5–10^6 m^{-1} in epitaxial ferroelectric thin films made of $HoMnO_3$. These results imply that the strain gradient generated in the thin film will induce a tremendous dielectric polarization of 10^{-4} C $m^{-1} \times 10^4$ $m^{-1} = 1$ C m^{-2} through flexoelectric coupling if we assume that the flexoelectric coefficient of the material does not change during the scaling down of the dimensions, say on the order of 10^{-4} C m^{-1}.[7] As a consequence, the very small flexoelectric polarization exhibited in bulk structures will become dramatically large in thin film systems. If this is true, the giant flexoelectric polarization will be significant and can be directly utilized in miniaturized devices, such as microelectromechanical system (MEMS) devices.

Unfortunately, the direct coupling between the macroscopic strain gradient and the polarization in ferroelectric thin film systems, as well as the flexoelectric coefficient of thin films, has never been reported. Although the giant elastic strain gradient[18,19] and the related polarization imprint and switching behaviors are confirmed to exist in ferroelectric thin films,[19,20] no direct experimental evidence has shown to date that the observed polarization in ferroelectric thin films comes partially from the strain gradient. In other words, no results clearly differentiate the contribution of flexoelectric polarization from that of ferroelectric polarization in ferroelectric thin films. In his recent work, Catalan[4] demonstrated that a horizontal strain gradient near the domain wall forces out-of-plane spontaneous polarization in the c domains to rotate away from the normal direction. Very recently, Lu and co-workers[21] reported that the strain gradients generated by the tip of a piezoresponse force microscope can completely reverse the orientation of the local polarization in an ultrathin epitaxial $BaTiO_3$ film, which directly demonstrated that flexoelectricity could dominate in nanoscale system. Here, we report that macroscopic strain gradiant can induce substantial flexoelectric polarization in a bent $Pb(Zr_{0.52}Ti_{0.48})O_3$ (PZT) diaphragm fabricated by micromachining and that this giant flexoelectric polarization can reverse the remnant ferroelectric polarization in PZT thin film.

A micromachined diaphragm has two obvious advantages in an investigation of flexoelectric polarization. First, the strain gradient can be quantified by observing the curvature of the diaphragm. Second, the state of the static polarization of the film can be evaluated by using the impedance-frequency spectrum in the vicinity of the resonant frequency. In principle, the Sawyer-Tower technique and the virtual ground method are not capable of measuring the initial/static values of the polarization since these methods rely on the measurement of switching charges when the polarization is changed by an external field. Measuring static polarization remains a difficult if not impossible task. Thanks to the micromachined diaphragm used in this study, it is possible to measure static polarization using normal polarization measurement methods. If electrical polarization exists in the film, the electromechanical coupling of the diaphragm at its resonant frequency can clearly show the polarization state. This indirect method suggests a new way to test the static/initial electrical polarization. With this method, the initial polarization induced by the strain gradient and the polarization switching behaviors in response to the external electric field are investigated systematically. The strain gradient induced by bending the diaphragm has been observed on the order of 10^2 m^{-1}, much larger than the strain gradient obtained in the bulk material. The observed giant flexoelectric polarization turns out to be on the same order of magnitude as the remnant polarization of the PZT film.

2. Results

To investigate flexoelectric polarization, it is important to get a bent diaphragm as the testing sample. Fortunately, stress usually accompanies the microfabrication process such that whenever there is a stress in the diaphragm, bending will be inevitable. As such, two kinds of bent diaphragms, PZT on SiO_2 and PZT on Si, were utilized in our experiment. We first selected a SiO_2 layer as the substrate of the diaphragm because it was subjected to compressive stress after growth. This compressive stress, together with a tensile stress in the PZT film after annealing, will induce a large strain gradient across the PZT film and thus ensure the bending of the diaphragm. This idea was confirmed by the observation that all our fabricated PZT/SiO_2 diaphragms were bent upward after fabrication. In fabricating the PZT/Si diaphragms, on the other hand, in addition to well-bent specimens, we obtained some very flat diaphragms with high tensile stress due to an unforeseen non-uniform stress distribution in the silicon on insulator (SOI) wafers. Sol-gel PZT film was used to investigate the flexoelectric effect because it has relatively high dielectric susceptibility among the known film families. The high susceptibility is closely associated with the high flexoelectric coefficient. **Figure 1** shows the schematic structure and dimensions of the PZT/Si diaphragm.

2.1. Bending of the Diaphragm and Self Polarization

After being released by deep reactive ion etching, the PZT/Si diaphragm has a convex profile (see Supporting Information, Figure S1) and bends upward (towards the top electrode) due to the stress in the multilayers, indicating a uniform strain gradient within the diaphragm,

$$\frac{\partial S_{11}}{\partial x_s} = \frac{1}{R} \tag{3}$$

where the radius of curvature, R, can be calculated from the measured central deflection height, h, and the radius, r, of the diaphragm.

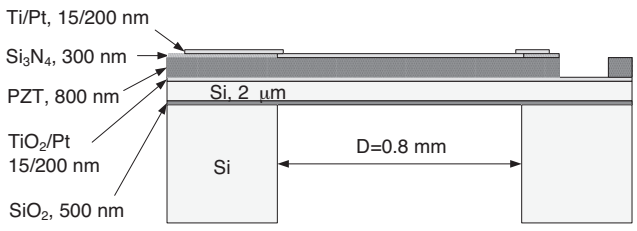

Figure 1. Schematic multilayer structure of the micromachined circular PZT/Si diaphragm used in this work.

Whenever there is polarization in the film, no matter its nature, electromechanical coupling can be induced by slight excitation with AC voltage. This coupling, as a measure of the polarization state of the film, can be observed through the impedance-frequency spectrum of the diaphragm. We measured the impedance spectra of the diaphragms that had not yet been subject to an external field. The results show that accompanying the bending of the as-released diaphragm, the PZT layers in both PZT/Si (**Figure 2**) and PZT/SiO_2 (see Supporting Information, Figure S2) diaphragms exhibit self-polarization. This is confirmed by occurrence of the resonant peaks in the impedance-frequency spectra. In Figure 2, a positive 1 V bias enhances the electromechanical response of the PZT/Si diaphragm, as indicated by the shift of the resonant peak and increased peak height of the phase angle at the resonant frequency. After removing the bias, the polarization state of the initial diaphragm is completely recovered. This result suggests that: 1) self-polarization exists in the as-fabricated dome-shaped diaphragm and 2) the polarization can be altered by applying DC bias. Next, we will consider from where this polarization originates, to where it directs, and how it varies with the applied bias.

2.2. Reversed Remnant Polarization and the Origin of the Self-Polarization

Electrically biasing the diaphragm may change the polarization state of the PZT film and generate stress (or strain) in the film plane, which will alter the curvature, the electromechanical coupling and the resonant frequency of the diaphragm. Therefore, by applying DC bias, we can study the development of the polarization in the diaphragm.

To estimate the quantitative magnitude of the polarization, the radius of curvature, and the coerceive electric field, we analyzed the PZT/Si diaphragm as shown in Figure 2. After removing the positive 1 V bias, a series of negative biases were applied to the diaphragm in a step-by-step fashion. A –1 V bias was first applied and then removed after recording the impedance spectrum and static surface profile. Thereafter, the cases of stronger negative biases were investigated successively. **Figure 3** shows the phase angle spectra at different negative biases. Because the negative voltage was applied to the top electrode during the testing, the applied electric field was directed from the bottom electrode to the top electrode. Figure 3a shows that the resonant peak decreases with increasing negative bias, indicating that the ferroelectric polarization induced by the negative bias counteracts the positive self-polarization. The self-polarization is directed from the top to the bottom electrode.

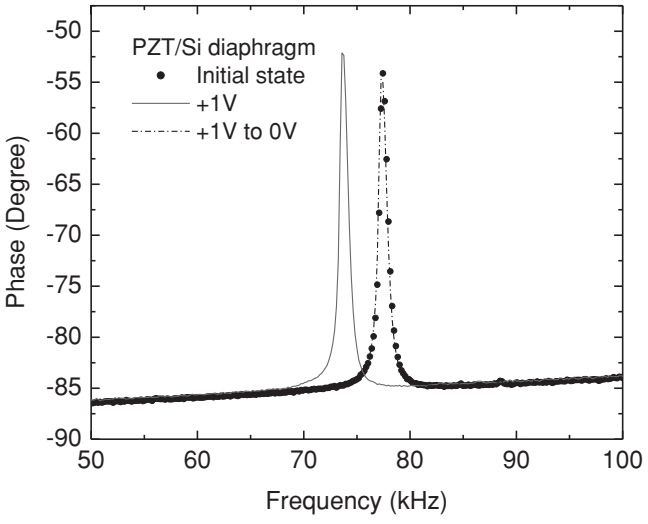

Figure 2. Phase-frequency spectra of the same circular PZT/Si diaphragm as shown in Figure 1. The resonant peak indicates that self-polarization exists in the PZT film on the as-fabricated bent diaphragm.

We can also see in Figure 3a that at –4 V bias, the resonant peak disappears. It is reasonable to suppose that, at this bias, the polarization in the film becomes zero and the –4 V becomes a negative coercive voltage. After removing the –4 V bias, part of the polarization was recovered as shown by the reappearance of resonant peak.

When the negative bias was increased continuously to –4.5 V and then –5 V, the resonant peak appeared again (Figure 3b) and the peak height increased with increasing bias. The resonant peak indicates that new polarization is generated in the diaphragm by the negative bias. At –5 V bias, the resulting negative polarization is larger than the remnant polarization after the –4 V bias is removed. Moreover, after removing the –5 V bias, the remnant polarization becomes zero as indicated by the disappearance of the resonant peak. Thus, we can expect that the remnant polarization after removing –4.5 V bias has switched back to the original positive direction. In other words, the negative polarization has a positive remnant polarization. We also observed this reversed remnant polarization in the PZT/SiO_2 diaphragm (see Supporting Information, Figure S3), indicating the possibility that this phenomenon is intrinsic in bent diaphragms.

The observed phenomenon suggests that, in addition to the bias, there must be another physical parameter that also affects the remnant polarization in this diaphragm system. We believe that the stress in the diaphragm plays this important role. The curvature of the diaphragm can be deformed by applying bias, but after removing the bias, the original curvature of the diaphragm is recovered due to the internal stress. The most reasonable explanation for the reversed remnant polarization is that the negative remnant ferroelectric polarization induced by the negative bias is smaller than the positive flexoelectric polarization induced by curvature of the diaphragm, thus causing the sum of the two components of the polarization to become positive. It is the curvature or the strain gradient of the diaphragm that forces the negative remnant polarization to switch to the positive direction! We believe that this reversed remnant polarization is direct evidence demonstrating that flexoelectric polarization exists in a curved PZT diaphragm.

To locate the origin of the self-polarization in the dome-shaped PZT diaphragm, we must mention another important observation in flat PZT/Si diaphragms with very high tensile stress. PZT films subjected to high tensile stress exhibit normal polarization-electric field (*P-E*) hysteresis loops but with relatively low relaxed remnant polarization. Even after long poling times at high voltage, these diaphragms do not exhibit resonant

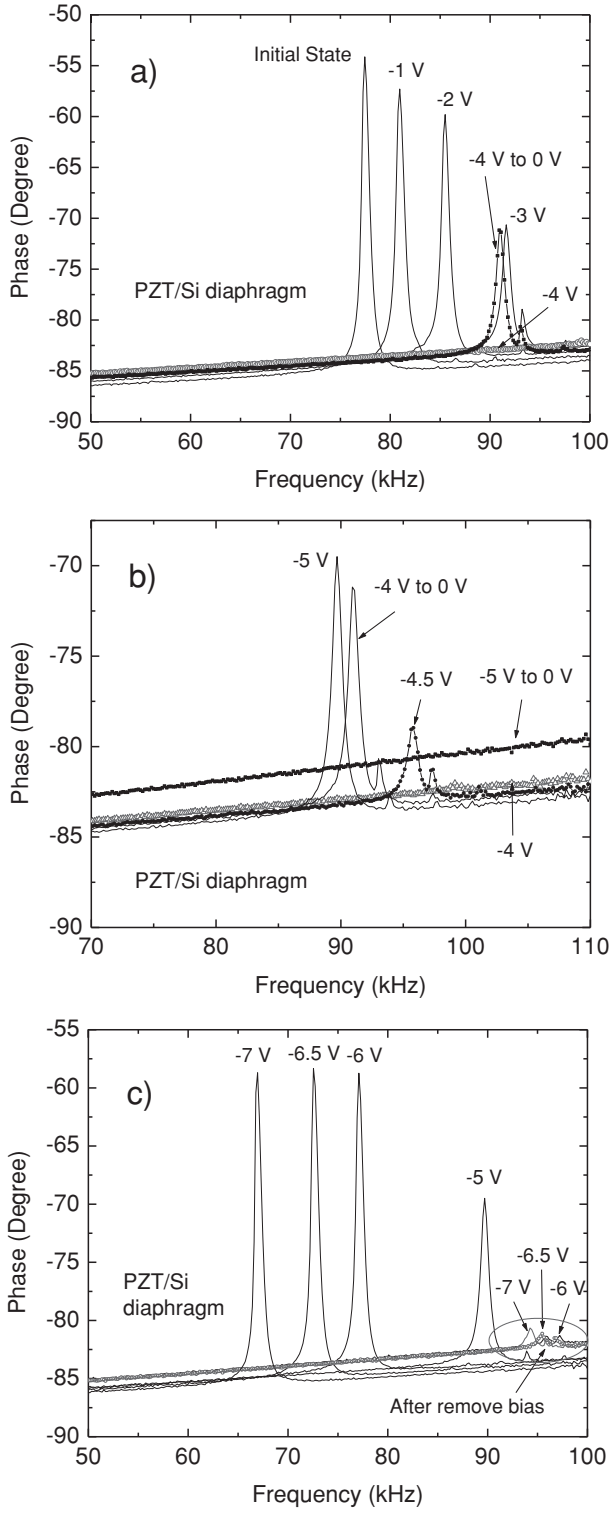

Figure 3. The effect of negative biases on phase-frequency spectra of the PZT/Si diaphragm. a) The negative bias increases gradually from −1 V to −4 V; the initial state is also shown for reference. b) The bias is increased to −5 V. c) The bias is further increased to −7 V.

peaks within a very broad frequency range in the impedance spectra revealing that flat PZT films subjected to high tensile stress do not possess any remnant polarization even after poling. When we applied static air pressure from the backside of the diaphragm through a sealed chamber, accompanying the deflection of the diaphragm, a resonant peak emerged in the impedance spectrum and the peak height increased as the air pressure was increased, no matter whether positive or negative pressure was applied. It is thus evident that the curvature, i.e. strain gradient, in the diaphragm causes the polarization. We therefore posit that the initial self-polarization existing in the bent diaphragm originates from the flexoelectric effect. In fact, we also observed that the self-polarization in PZT films is always associated with the bending of the diaphragm.

Because the diaphragm was bent upward (Supporting Information, Figure S1), we noticed that the flexoelectric polarization induced by the strain gradient opposes the direction of the strain gradient.

Figure 3c shows that the reversed polarization increased dramatically when the bias was increased to −7 V. However, after removing this bias, the remnant polarization became unexpectedly small, which is evidenced in the very low resonant peak heights. Considering the remnant polarization was zero after removing the −5 V bias, the remnant polarization is maintained in the reverse direction.

After removing the −7 V bias, a series of positive biases were applied to the diaphragm. **Figure 4** shows the effect of the positive bias on the phase angle spectra. In Figure 4a we observe that, the very small remnant polarization caused by the −7 V bias can be totally counterbalanced by applying a 1 V positive bias, much smaller than the negative coercive voltage of −4 V. The polarization direction is also clearly reversed at 1.5 V and 2 V bias. Figure 4b shows that the positive polarization increased as the positive bias was increased. However, the resonant peaks decreased as the bias was increased when the bias was higher than 4 V. This is because the gradually saturated polarizations and increased stress above these positive voltages reduced the electromechanical coupling, just as the d_{33} coefficient decreases above a certain voltage in d_{33}-bias curves of normal ferroelectric films. When the bias increased from 6 V to 7 V, the resonant frequency increased because the ferroelectric polarization induced by the bias flattens the dome and thus generates higher stress in the diaphragm. Figure 4c clearly shows that after removing the positive bias, the positive remnant polarization is much larger than the negative one. The remnant polarization is therefore asymmetric. Asymmetric remnant polarization was also observed in the PZT/SiO_2 diaphragm (see Supporting Information, Figure S3c).

Gruverman et al.[20] reported that bending the substrate strongly shifts the P-E hysteresis loops of PZT thin film capacitors. As a result, the PZT film is in a single domain polarization state. The polarization direction can be easily reversed by changing the direction of the bending of the substrate. However, even after application of an opposite poling voltage, the polarization switches back to its original direction. It is therefore not the poling voltage but the substrate bending that dominates the polarization state. Lee et al.[19] demonstrated that the strain gradient in the thin film results in a shift in the hysteresis loop. The above mentioned observations imply that the shift in the hysteresis loops must be strongly related to the flexoelectric effect. In our PZT/Si diaphragm, the curvature of the diaphragm partially recovers to its original state when the bias is

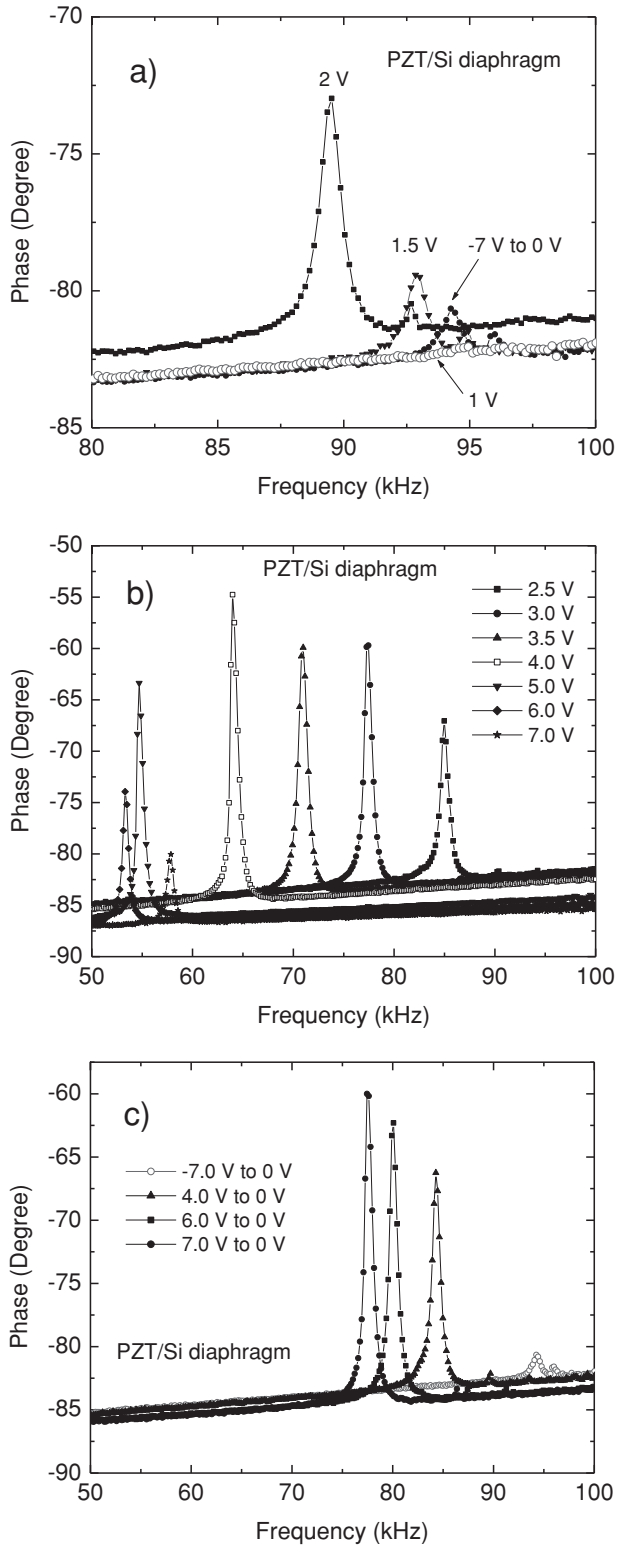

Figure 4. The effect of positive biases on phase-frequency spectra of the PZT/Si diaphragm. a) The negative remnant polarization is completely counterbalanced at a positive bias of 1 V. b) The positive polarization increases with additional increases of the positive bias. c) The positive remnant polarization is much larger than the negative one.

removed due to internal stress and flexoelectric polarization is generated. It is obvious that the flexoelectric polarization due to the shape of the diaphragm counterbalances the negative remnant ferroelectric polarization and enhances the positive polarizations. This is why the *P-E* hysteresis is asymmetric.

2.3. Central Deflection and Radius of the Curvature in Relation to the External Bias

During the measurement of the impedance frequency spectra, the static surface profiles of the diaphragm were also measured at each applied bias. Correlations between the diaphragm curvature and the polarization enable us to investigate the flexoelectric effect. **Figure 5** shows the measured relations between the static central deflection of the diaphragm and the bias. The solid circles show the central deflection at particular biases. The hollow circles and squares indicate the deflection after removing the bias. We can clearly see that starting from the original state, the central deflection increases as the negative bias is increased and reaches its maximum at −4 V. Any further increase in the bias reduces the dome height. However, when the −7 V bias is removed, the central deflection is higher than the original deflection. While increasing the positive bias, the deflection height increases a little and reaches its maximum at 1 V. When the positive bias is continuously increased, the central deflection decreases. It is evident that the central deflection has a close correlation with the impedance results shown in Figure 3 and 4. The maximum central deflection corresponds to the zero electromechanical coupling and thus to the coercive voltage.

The increased deflection height implies an increase in the flexoelectric polarization. Considering that flexoelectric polarization is opposite to ferroelectric polarization induced by the negative bias, the negative bias first needs to counterbalance the gradually increased flexoelectric polarization. Higher voltage is

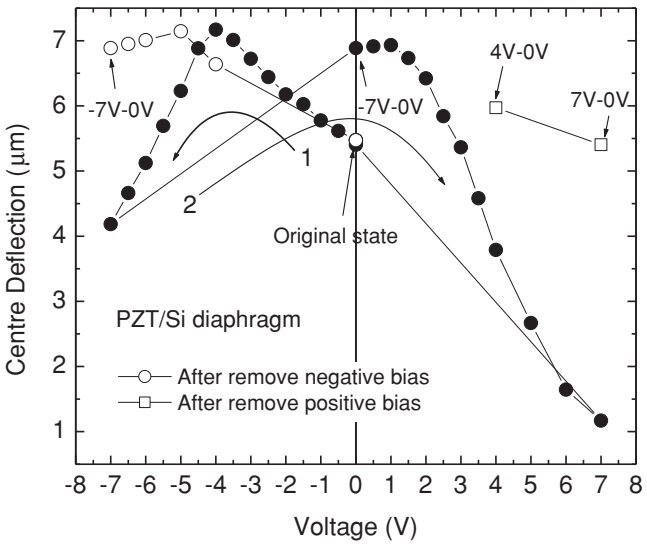

Figure 5. The bias dependence of the central deflection of the PZT/Si diaphragm.

Table 1. Estimated flexoelectric polarization from the tested curvature radius of the PZT/Si diaphragm at $\mu_{12} = 2.13 \times 10^{-4}$ C m^{-1}.

Voltage [V]	Initial 0	−4	−7	−7 to 0	1	7	7 to 0
h [μm]	5.473	7.170	4.184	6.886	6.933	1.168	5.403
R [m]	0.0146	0.0112	0.0191	0.0116	0.0115	0.0685	0.0148
CV/A [μC cm^{-2}]	0	−4.96	−6.27	0	1.21	5.29	0
P^{flexo} [μC cm^{-2}]	1.46	1.90	1.11	1.83	1.85	0.311	1.44

thus needed to fully counterbalance the positive polarization, including both the ferroelectric and flexoelectric components. Beyond the −4 V coercive voltage, the reoccurrence of the negative polarization generates tensile stress within the PZT film and thus reduces the deflection height. Upon removing the −7 V bias, the diaphragm rebounds to a higher dome height, such that the relatively larger flexoelectric polarization counterbalances part of the ferroelectric remnant polarization, resulting in a very small negative remnant polarization. Further application of the positive bias together with the positive flexoelectric polarization can reverse the negative remnant polarization very easily. This is why the deflection-voltage hysteresis loop shifts to the negative voltage side. Beyond a positive coercive voltage of 1 V, the gradually increased positive polarization flattens the diaphragm again and thus reduces the flexoelectric polarization. However, because the flexoelectric polarization is parallel to the positive ferroelectric polarization, the sum of the two components still gives a relatively large positive polarization, and therefore a large positive remnant polarization after removing +7 V bias.

For a dome-shaped diaphragm with radius of r, the radius of curvature, R, and the central deflection height, h, has the relation

$$R = \frac{r^2}{2h} \tag{4}$$

assuming that $h << r$. The calculated R's of the points of interest are summarized in **Table 1**.

2.4. Asymmetric *C-V* Curve

After testing the impedance and surface profile of the diaphragm, the *C-V* curve was tested at 1 kHz. **Figure 6** shows that when the bias varies from +7 V to −7 V, the capacitance first increases to a maximum of 6.23 nF at −3.01 V and then decreases. When the voltage is increased from −7 V to 7 V, the maximum capacitance occurs at 1.26 V. When the +7 V bias is removed, the capacitance of the diaphragm goes back to around 5.40 nF. The flat C-V curve was measured at 0 V bias for a period of time by switching off the bias while still setting to sweep it from +7 V to −7 V. No bias was really applied to the diaphragm during test. It is clear that the *C-V* curve has similar asymmetric features as the deflection-bias loop. It also shifts to negative voltage side.

The dielectric loss of the PZT film (see Supporting Information, Figure S4) was also measured simultaneously with the

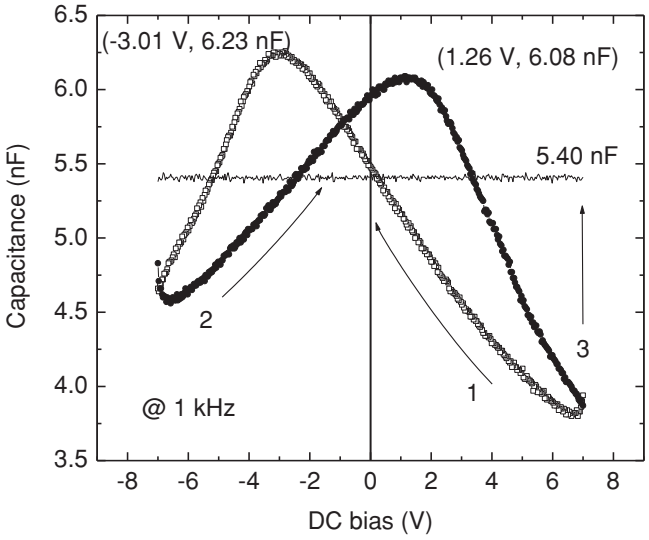

Figure 6. *C-V* curves of the PZT/Si diaphragm.

C-V curve. The tested data (ranged from 0.045 to 0.075) is among the typical values of PZT thin films. The *I-V* curve in Figure S5 (Supporting Information) shows the electrical conductance G of the PZT/Si diaphragm is 6.99×10^{-10} S. The maximum non-ferroelectric charge density caused by dielectric loss during the *P-E* test is thus estimated as less than 0.24 nC cm^{-2}. In comparison with the magnitude of ferroelectric polarization (on the order of μC cm^{-2}), the dielectric loss induced charge in our PZT film can be neglected.

2.5. *P-E* Hysteresis-Start from Absolute Zero Polarization

As mentioned above, the normal dynamic polarization measurement methods alone are not capable of testing the static polarization due to lack of a reference point. Fortunately, the electromechanical coupling of a diaphragm obtained from impedance spectrum provides us with a right reference. We can tell from Figure 3b that after removing the −5 V bias the polarization in the film is absolute zero. Starting from this point, without applying a preset voltage cycle we can obtain an absolute *P-E* hysteresis loop start from absolute zero polarization, which indicates the real polarization at every test points. The result was shown in **Figure 7** as curve 1. It is evident that within the small testing voltage range the P-E hysteresis is absolutely not symmetric. The positive P_r (5.10 μC cm^{-2}) is larger than negative P_r (−4.14 μC cm^{-2}) and the negative V_c is −2.70 V. After that the test was repeated with a preset voltage circle to ensure the first leg of the loop starts from negative polarization state. The results were recorded as a non-centered curve 2. Since we did not change the maximum voltage, the P_r and P_{max} of the *P-E* hysteresis would not change. Shifting the curve by aligning the $+P_r$ with that of curve 1 we get curve 3 from which we can obtain $+V_c$ equals 1.49 V, and the relaxed negative remnant polarization is −2.90 μC cm^{-2}. Curve 3 gives the absolute polarization for every test points. We can see from curve 3 that both coercive field and remnant polarization of the

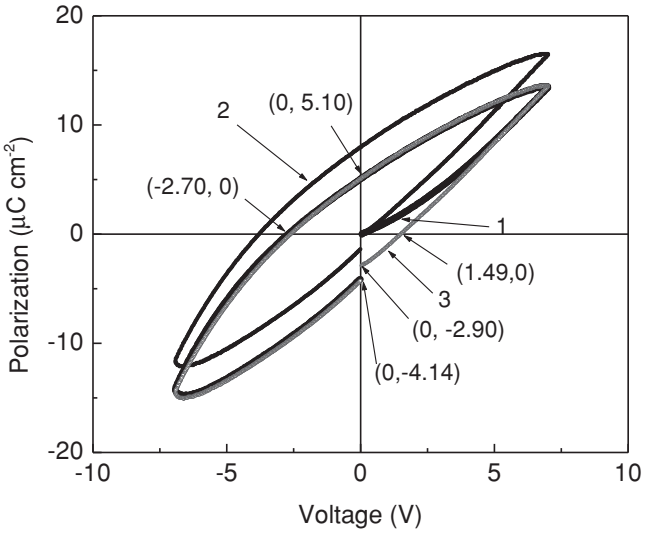

Figure 7. *P-E* hysteresis of PZT/Si diaphragm measured by normal virtual ground method. The film was depolarized at −5 V from positive remnant polarization state. The real zero polarization state of curve 1 was verified using impedance spectrum.

film are not symmetric. The *P-E* curves at high voltages were also measured as shown in Figure S6 (Supporting Information). It is clear from Figure S6 (Supporting Information) that the "banana shape" of the *P-E* hysteresis at ±7 V is due to lack of saturation.

3. Estimation of the Flexoelectric Coefficient

With the experimental data obtained here, we can calculate the flexoelectric coefficient of PZT film by analyzing the polarization components. It should be pointed out that the origin of the self-polarization and build-in bias is very complicated. Asymmetric nature of top and bottom electrode, aligned defect dipoles, different grain shapes and strain gradient are all the possible sources. In order to simplify the analysis, only the strain gradient is considered in the following analytical model. Since the other factors have been excluded, the obtained results estimate the upper bound of flexoelectric coefficient based on the assumption that the other factors are quantitatively less important.

In a non-zero field, *E*, the constitutive equation for direct flexoelectricity takes the form

$$P = \varepsilon_0 \chi E + \mu_{12} \frac{\partial S_{11}}{\partial x_s} \approx \varepsilon_0 \varepsilon_r E + \mu_{12} \frac{1}{R} = \frac{CV}{A} + \mu_{12} \frac{1}{R} \quad (5)$$

where P is the polarization, χ the dielectric susceptibility, R the radius of curvature of the diaphragm, ε_r the relative dielectric constant, C the capacitance and A the area of the diaphragm. In the bent diaphragm geometry, the strain gradient is normal to the film plane and equals $1/R$. For films with high dielectric susceptibility, $\varepsilon_r = 1 + \chi \approx \chi$.

Since PZT is also a ferroelectric material, in a small field range within the coercive field, the remnant ferroelectric polarization is initially pronounced and should also be taken into account. Therefore,

$$P = P_r^{ferro} + P^{piezo} + \varepsilon_0 \chi E + P^{flexo} \approx P_r^{ferro} + P^{piezo} + \frac{CV}{A} + \mu_{12} \frac{1}{R} \quad (6)$$

where P_r^{ferro} is the remnant ferroelectric polarization and P^{piezo} is the contribution of conventional piezoelectricity to the polarization. If $P > 0$, the strain in the film will induce P^{piezo} through piezoelectric stress coefficient e_{31}. The remnant P_r^{ferro} can be considered as a constant which is determined by the highest external field, E_{max}, while testing the P-E loop. The first three terms on the right side of Equation (6) contribute to the hysteresis and nonlinearity of the *P-E* loop, while the last term contributes to the asymmetric feature of the P-E loop. The above equation holds only in a small voltage range. The effect of P_r^{ferro} may vanish beyond the coercive voltage.

From Figures 3b, 4a and 5, we can see that at $V = -4$ V and $V = 1$ V, the polarization, P, is 0. Thus, the contribution from piezoelectricity at these two coercive voltages also becomes zero, i.e., $P^{piezo} = 0$. We can therefore obtain

$$P_r^{ferro} - \frac{4C_{-4}}{A} + \mu_{12} \frac{1}{R_{-4}} = 0 \quad (7)$$

$$-P_r^{ferro} + \frac{C_1}{A} + \mu_{12} \frac{1}{R_1} = 0 \quad (8)$$

The capacitances at the two coercive voltages (C_{-4} = 6.23 nF and C_1 = 6.08 nF) are known from the *C-V* curve shown in Figure 6. The radius of curvature is already obtained from the dome-shaped diaphragm, as listed in Table 1. The diameter of the diaphragm is 0.8 mm. Solving the above equations, we obtain

$$\mu_{12} = 2.13 \times 10^{-4} \text{C m}^{-1} \quad (9)$$

$$P_r^{ferro} = 3.06 \times 10^{-2} \text{C m}^{-2} = 3.06\, \mu\text{C cm}^{-2} \quad (10)$$

It should be pointed out that the coercive voltage obtained from the *C-V* curve (Figure 6) is different from that obtained from the impedance measurement (Figure 3b, 4a and 5). The possible reason is that the *C-V* test is completed within seconds thus has relatively high frequency of bias loop, while the impedance spectrum is obtained at a certain DC bias. It takes minutes to obtain the impedance spectrum at each DC bias. Therefore, the difference in coercive voltage between those obtained from impedance measurement and *C-V* test can be attributed to the relaxation of strain and polarization in the diaphragm during the impedance measurement. Nevertheless, using the capacitance data at coercive voltage (the two peak values in Figure 6) instead of the data at −4 V and +1 V in *C-V* curve is reasonable and should be reasonably accurate.

Counting in the contribution of flexoelectric polarization at positive remnant state (1.44 μC cm^{-2}) and negative polarization state (1.83 μC cm^{-2}) in Table 1, the estimated nominal ferroelectric remnant polarization 3.06 μC cm^{-2} in Equation 10 gives the $+Pr$ of 4.50 μC cm^{-2} and $-Pr$ of 2.23 μC cm^{-2}, respectively. These results agree well with the measured remnant polarization (see Figure 7) in the order of magnitude.

It is worth mentioning that the contribution of flexoelectric polarization in Equation (6) shifts the *P-E* hysteresis loop along the *P* axis. *P* is no longer symmetric about the voltage axis. Because a reference polarization state is lacking, it is impossible to accurately locate the *P-E* hysteresis loop along the *P* axis and further to determine the static polarization value by using only conventional dynamic polarization measurement methods. The conventional Sawyer-Tower technique and the virtual ground method can only measure the shape of a *P-E* loop but these methods are not capable of indicating the exact location of the loop if the loop is not symmetric. Normally, the given values of the remnant polarization and the coercive field in the asymmetric loop are not accurate. Unfortunately, this point is neglected in most of the published work when dealing with asymmetric *P-E* loops. On the contrary, the electromechanical coupling method accurately determines the coercive field, which enables us to calculate the contribution of the flexoelectric polarization accurately.

The calculated value of the norminal remnant polarization is smaller than the normal value for PZT films. However, this result is reasonable considering that the tests were conducted in a small field range (±7 V) in which the polarization was not fully saturated (see Supporting Information, Figure S6).

It can be seen from Table 1 that the initial self-polarization induced by the strain gradient at 0 V is 1.46 μC cm^{-2}, and the flexoelectric polarization at −4 V is 1.90 μC cm^{-2}. These giant flexoelectric polarization values confirm our prediction that the flexoelectric polarization in thin film systems can be dramatically large; indeed, they are on the same order of magnitude as the normal remnant ferroelectric polarization of PZT film.

In addition to the analysis based on polarization, we can also estimate the flexoelectric coefficient from the internal electric field induced by the flexoelecric effect and the observed coercive electric field. A pure ferroelectric *P-E* loop is symmetric. We can thus define a coercive electric field for ferroelectricity, E_c^{ferro}, which is a constant for a given maximum external electric field. Flexoelectric polarization generates an equivalent internal electric field, E^{flexo}, which shifts the *P-E* loop along the *E*-axis. The real coercive field, E_c, in the resulting *P-E* loop will take the form

$$E_c = E_c^{ferro} + E^{flexo} \tag{11}$$

$$E^{flexo} = \frac{\mu_{12}}{\varepsilon_0 \chi}\frac{1}{R} \approx \frac{\mu_{12} A}{Ct}\frac{1}{R} \tag{12}$$

where A is the area of the diaphragm/capacitor and $t = 0.8 \times 10^{-6}$ m is the thickness of the PZT film. Again, using the test data in Figure 5 and 6 and Table 1 at coercive voltages of −4 V and 1 V, we obtain

$$\frac{-4}{0.8 \times 10^{-6}} = -E_c^{ferro} - \frac{\mu_{12} A}{0.8 \times 10^{-6} C_{-4}}\frac{1}{R_{-4}} \tag{13}$$

$$\frac{1}{0.8 \times 10^{-6}} = E_c^{ferro} - \frac{\mu_{12} A}{0.8 \times 10^{-6} C_1}\frac{1}{R_1} \tag{14}$$

Solving Equations (13) and (14), we obtain

$$\mu_{12} = 2.08 \times 10^{-4}\,\mathrm{C\,m^{-1}} \tag{15}$$

$$E_c^{ferro} = 3.12\ \mathrm{MV\,m^{-1}} \tag{16}$$

The equivalent internal electric field induced by flexoelectricity at −4 V is

$$E_{-4}^{flexo} = 1.88\ \mathrm{MV\,m^{-1}} \tag{17}$$

By comparing Equations (9) and (15), we can see that the two methods give the same flexoelectric coefficient value, suggesting that the proposed model explains the observed reversed remnant polarization phenomenon in piezoelectric diaphragms with flexoelectric effects. The flexoelectric effect shifts the *P-E* hysteresis loop not only along the *E*-axis but also along the *P*-axis. This result agrees well with the measured *P-E* hysteresis loop as shown in Figure 7. The phenomenon of self-polarization[22–25] has been observed in various ferroelectric thin films for decades. As has been already pointed out in previous work,[19,20] our work also demonstrated that strain gradient can induce self-polarization and thus is one of the sources of the built-in bias.

The obtained flexoelectric coefficient μ_{12} in PZT thin films is on the order of 10^{-4} C m^{-1}. This value is surprisingly high as it is two orders of magnitude greater than the reported value for PZT bulk ceramics.[10] However, this value is on the same order of magnitude as that measured in $Ba_{0.67}Sr_{0.33}TiO_3$ ceramics,[7] which has the highest flexoelectric coefficient, μ_{12}, among the reported high-susceptibility ferroelectric ceramics.

4. Conclusions

The polarization induced by the strain gradient, i.e., the flexoelectric effect, has been directly observed in bent PZT diaphragms. Observation of the electromechanical coupling of a ferroelectric diaphragm has revealed a new way to test the static electrical polarization state. This method makes it possible to determine accurately the coercive electric field at which the polarization is truly zero. The strain gradient induced in a dome-shaped micromachined PZT diaphragm is measured to be on the order of 10^2 m^{-1}, much larger than that obtained in the bulk material. From the measured coercive electric field and the strain gradient, the flexoelectric coefficient of PZT thin films is estimated to be 2.0×10^{-4} C m^{-1}. The large strain gradient together with the high flexoelectric coefficient generates giant flexoelectric polarization on the order of 1 μC cm^{-2}, which is comparable to the remnant ferroelectric polarization of PZT thin films.

5. Experimental Section

The fabrication process of the PZT/Si diaphragms is depicted in Figure 1. A <100> SOI wafer with a 2 μm device layer was used as the substrate. Firstly, thin TiO_2/Pt (15 nm/200 nm) films were deposited as the bottom electrode by sputtering. Secondly, a thin $Pb(Zr_{0.52}Ti_{0.48})O_3$ film (≈0.8 μm) was deposited by the sol-gel deposition technique. To open access to the bottom electrode pad, in the third step, the PZT film was wet etched in diluted HCl:HF solution. Afterwards, a Si_3N_4 layer (300 nm) was deposited by plasma-enhanced chemical vapor deposition (PECVD) and patterned by reactive ion etching (RIE) to serve as an insulation layer to minimize parasitic capacitance induced by the patterned electrode

wiring. The top Ti/Pt (15 nm/200 nm) electrode was sputtered and patterned by using the lift-off technique. Finally, the diaphragm was released by deep reactive ion etching (DRIE). The diameter of the diaphragm was 0.8 mm.

The static profile of the released diaphragm was measured by using a 3D-view digital holographic interferometer.[26] An Agilent 4294A impedance analyzer was used to test the impedance spectrum and the *C-V* curves of the diaphragm. To maintain consistency in the results, during the testing, the high voltage port of the Agilent 4294A impedance analyzer was always connected to the top electrode of the diaphragm. The DC bias and AC driving signal were applied to the diaphragm through the impedance analyzer. The oscillation AC level of the activating voltage was 5 mV. The impedance frequency spectra at different DC biases were measured in both the "bias on" and "bias off" states. At each applied bias, we recorded the first spectrum while the bias was applied, followed by the measurement of the diaphragm profile. After the bias was removed, we recorded the second surface profile and the spectrum, which exhibited the remnant polarization state. Instead of impedance magnitudes, phase shifts were used to qualitatively measure the polarization within the film because these parameters were more pronounced. The *C-V* curve was recorded separately after we finished the impedance tests at all the biases. *P-E* hysteresis was measured using Precision Pro ferroelectric analyzer (Radiant Technology Inc., Albuquerque, NM).

Supporting Information

Supporting Information is available from the Wiley Online Library or from the author.

Acknowledgements

The authors would like to thank Professor X. Yao and Professor L. E. Cross for valuable discussions that inspired this work, Dr. V. R. Singh for help with the holographic profile measurement, and Dr. T. Xu for help with the fabrication of the PZT diaphragms.

Received: March 25, 2012
Revised: June 29, 2012
Published online: August 13, 2012

[1] K. J. Choi, M. Biegalski, Y. L. Li, A. Sharan, J. Schubert, R. Uecker, P. Reiche, Y. B. Chen, X. Q. Pan, V. Gopalan, L. Q. Chen, D. G. Schlom, C. B. Eom, *Science* **2004**, *306*, 1005.
[2] J. H. Haeni, P. Irvin, W. Chang, R. Uecker, P. Reiche, Y. L. Li, S. Choudhury, W. Tian, M. E. Hawley, B. Craigo, A. K. Tagantsev, X. Q. Pan, S. K. Streiffer, L. Q. Chen, S. W. Kirchoefer, J. Levy, D. G. Schlom, *Nature* **2004**, *430*, 758.
[3] M. P. Warusawithana, C. Cen, C. R. Sleasman, J. C. Woicik, Y. L. Li, L. F. Kourkoutis, J. A. Klug, H. Li, P. Ryan, L. P. Wang, M. Bedzyk, D. A. Muller, L. Q. Chen, J. Levy, D. G. Schlom, *Science* **2009**, *324*, 367.
[4] G. Catalan, A. Lubk, A. H. G. Vlooswijk, E. Snoeck, C. Magen, A. Janssens, G. Rispens, G. Rijnders, D. H. A. Blank, B. Noheda, *Nat. Mater.* **2011**, *10*, 963.
[5] A. K. Tagantsev, *Phys. Rev. B* **1986**, *34*, 5883.
[6] L. E. Cross, *J. Mater. Sci.* **2006**, *41*, 53.
[7] W. H. Ma, L. E. Cross, *Appl. Phys. Lett.* **2002**, *81*, 3440.
[8] W. H. Ma, L. E. Cross, *Appl. Phys. Lett.* **2006**, *88*, 232902.
[9] W. H. Ma, L. E. Cross, *Appl. Phys. Lett.* **2003**, *82*, 3293.
[10] W. H. Ma, L. E. Cross, *Appl. Phys. Lett.* **2005**, *86*, 072905.
[11] W. H. Ma, L. E. Cross, *Appl. Phys. Lett.* **2001**, *79*, 4420.
[12] W. H. Ma, L. E. Cross, *Appl Phys Lett* **2001**, *78*, 2920.
[13] P. Zubko, G. Catalan, A. Buckley, P. R. L. Welche, J. F. Scott, *Phys. Rev. Lett.* **2007**, *99*, 167601.
[14] G. Catalan, L. J. Sinnamon, J. M. Gregg, *J. Phys.-Condes. Matter* **2004**, *16*, 2253.
[15] J. W. Hong, G. Catalan, J. F. Scott, E. Artacho, *J. Phys.-Condes. Matter* **2010**, *22*, 112201.
[16] R. Resta, *Phys. Rev. Lett.* **2010**, *105*, 127601.
[17] R. Maranganti, P. Sharma, *Phys. Rev. B* **2009**, *80*, 054109.
[18] G. Catalan, B. Noheda, J. McAneney, L. J. Sinnamon, J. M. Gregg, *Phys. Rev. B* **2005**, *72*, 020102.
[19] D. Lee, A. Yoon, S. Y. Jang, J. G. Yoon, J. S. Chung, M. Kim, J. F. Scott, T. W. Noh, *Phys. Rev. Lett.* **2011**, *107*, 057602.
[20] A. Gruverman, B. J. Rodriguez, A. I. Kingon, R. J. Nemanich, A. K. Tagantsev, J. S. Cross, M. Tsukada, *Appl. Phys. Lett.* **2003**, *83*, 728.
[21] H. Lu, C.-W. Bark, D. Esque de los Ojos, J. Alcala, C. B. Eom, G. Catalan, A. Gruverman, *Science* **2012**, *336*, 59.
[22] E. Sviridov, I. Sem, V. Alyoshin, S. Biryukov, V. Dudkevich, *Mater. Res. Soc. Symp. Proc.* **1995**, *361*, 141.
[23] A. L. Kholkin, K. G. Brooks, D. V. Taylor, S. Hiboux, N. Setter, *Integr. Ferroelectr.* **1998**, *22*, 1045.
[24] S. Sun, Y. M. Wang, P. A. Fuierer, B. A. Tuttle, *Integr. Ferroelectr.* **1999**, *23*, 25.
[25] V. P. Afanasjev, A. A. Petrov, I. P. Pronin, E. A. Tarakanov, E. J. Kaptelov, J. Graul, *J. Phys.-Condes. Matter* **2001**, *13*, 8755.
[26] V. R. Singh, J. M. Miao, Z. H. Wang, G. Hegde, A. Asundi, *Opt. Commun.* **2007**, *280*, 285.